Published in final edited form as:
Dev Biol. 2013 January 1; 373(1): 95–106. doi:10.1016/j.ydbio.2012.10.007.

BMP-binding protein Twisted gastrulation is required in mammary gland epithelium for normal ductal elongation and myoepithelial compartmentalization

Cynthia L. Forsman[1,2,3], **Brandon C. Ng**[1,2], **Rachel K. Heinze**[1,2], **Claire Kuo**[1,2], **Consolato Sergi**[4], **Rajaram Gopalakrishnan**[5], **Douglas Yee**[3,6], **Daniel Graf**[7], **Kathryn L. Schwertfeger**[3,8], and **Anna Petryk**[1,2,3,*]

[1]Department of Genetics, Cell Biology and Development, University of Minnesota, Minneapolis, MN 55455, USA [2]Department of Pediatrics, University of Minnesota, Minneapolis, MN 55455, USA [3]Masonic Cancer Center, University of Minnesota, Minneapolis, MN 55455, USA [4]Department of Laboratory Medicine & Pathology, University of Alberta, Alberta, Canada T6G 2B7 [5]Diagnostic/Biological Sciences, School of Dentistry, University of Minnesota, Minneapolis, MN 55455, USA [6]Department of Medicine, University of Minnesota Medical School, Minneapolis, Minnesota 55455, USA [7]Institute of Oral Biology, Faculty of Medicine, University of Zurich, Zurich, Switzerland [8]Department of Laboratory Medicine and Pathology, University of Minnesota, Minneapolis, MN 55455, USA

Abstract

Bone morphogenetic proteins (BMPs) are involved in embryonic mammary gland (MG) development and can be dysregulated in breast cancer. However, the role BMPs play in the postnatal MG remains virtually unknown. BMPs are potent morphogens that are involved in cell fate determination, proliferation, apoptosis and adult tissue homeostasis. Twisted gastrulation (TWSG1) is a secreted BMP binding protein that modulates BMP ligand availability in the extracellular space. Here we investigate the consequences of TWSG1 deletion on development of the postnatal MG. At puberty, *Twsg1* is expressed in the myoepithelium and in a subset of body cells of the terminal end buds. In the mature duct, *Twsg1* expression is primarily restricted to the myoepithelial layer. Global deletion of *Twsg1* leads to a delay in ductal elongation, reduced secondary branching, enlarged terminal end buds, and occluded lumens. This is associated with an increase in luminal epithelial cell number and a decrease in apoptosis. In the MG, pSMAD1/5/8 level and the expression of BMP target genes are reduced, consistent with a decrease in BMP signaling. GATA-3, which is required for luminal identity, is reduced in $Twsg1^{-/-}$ MGs, which may explain why K14 positive cells, which are normally restricted to the myoepithelial layer, are found within the luminal compartment and shed into the lumen. In summary, regulation of BMP signaling by TWSG1 is required for normal ductal elongation, branching of the ductal tree, lumen formation, and myoepithelial compartmentalization in the postnatal MG.

*To whom correspondence should be addressed: Dr. Anna Petryk, University of Minnesota, Department of Pediatrics, East Bldg Rm MB671, 2450 Riverside Ave., Minneapolis, MN 55454, Phone: 612-624-5409, Fax: 612-626-5262, petry005@umn.edu.

Keywords

TWSG1; BMP; mammary gland development; breast; myoepithelium

Introduction

Bone morphogenetic proteins (BMPs), members of the transforming growth factor 3 (TGF3) superfamily, are morphogens that play diverse roles during embryonic development and postnatal life (Wagner et al., 2010). BMPs have been implicated in regulating tissue homeostasis in physiological states as well as pathological ones, such as cancer, by mediating basic biological processes including cell proliferation, migration, differentiation, apoptosis, and epithelial-stromal interactions (Buijs et al., 2012; Singh and Morris, 2010; Virtanen et al., 2011; Wang et al., 2011a). There is growing evidence that developmental programs, which are important during embryonic development and adult homeostasis, can be inappropriately reactivated during the initiation and progression of cancer (Bowman and Nusse, 2011; McEvoy et al., 2011; Wang et al., 2011b). Specifically, BMPs play important roles during embryonic mammary gland (MG) development and have been shown to be dysregulated in breast and other cancers often acting as a tumor suppressor or tumor promoter depending on dosage, time and tissue of expression (Bailey et al., 2007; Beppu et al., 2008; Cho et al., 2006; Hens et al., 2007; Liu et al., 2008). Given that developmental programs, such as BMP mediated processes, are co-opted or exploited by tumorigenic cells, it is important to understand what roles BMPs play during normal MG development and how their activity is regulated.

In both humans and mice, the MG is a dynamic organ that responds and develops over the lifetime of the female. Embryonic development establishes the rudimentary ductal tree that during puberty, pregnancy and lactation undergoes complex morphological changes (Hens and Wysolmerski, 2005; Hovey and Trott, 2004). In the mouse, MG development begins around embryonic day 10.5 (E10.5) when epithelial thickenings form placodes, which further thicken and invaginate as they respond to inductive signals from the underlying mesenchyme at around E13.5. At approximately E16.5, the primary bud epithelium proliferates and elongates into the developing fat pad forming a rudimentary tree. Development is arrested at this point until puberty. At puberty, terminal end buds (TEBs) form at the leading edge of the duct and are the site of active proliferation and apoptosis (Dulbecco et al., 1982; Humphreys et al., 1996). The TEB consists of bipotent cap cells that generate both cytokeratin 18 (K18) positive luminal and K14 positive myoepithelial cells. The latter remain in contact with the extracellular matrix (ECM) while the luminal cells polarize with their apical aspect oriented towards the lumen. In the TEB, proliferation creates excess body cells, which generate the mass of the duct as it elongates and a subset these cells undergo apoptosis to form the lumen. Clearing of excess cells is complete and the mature ductal structure can be seen beginning at the shoulder of the TEB (Humphreys et al., 1996). A mature duct consists of a layer, one to two cells wide, of K18 positive luminal cells and a single cell layer of K14 positive myoepithelial basal cells. Once the ducts reach the edges of the fat pad, TEBs are reabsorbed and elongation ceases. Concomitant with elongation, the ductal tree is further elaborated by a tightly regulated process of secondary and tertiary branching.

The dynamic changes seen in the MG are regulated by morphogens (Jardé and Dale, 2012; Schwertfeger, 2009), cytokines/growth factors (McNally and Martin, 2011; Watson et al., 2011) and hormones (McNally and Martin, 2011). Integration and regulation of these signals is required for the proper establishment of the MG anlagen and subsequent development through puberty and pregnancy. Past studies have suggested that BMP 2 and 4 play a role

during MG development, including bud formation, epithelial mesenchymal communication, proliferation and lumen formation (Hens et al., 2007; Montesano, 2007; Phippard et al., 1996; van Genderen et al., 1994), but understanding of the regulation of BMP signaling during MG development is limited.

The BMP specific intracellular signal transducers of BMPs are SMAD1/5/8 proteins, which become phosphorylated upon binding of BMPs (BMP 2, 4, 6 or 7 among others) to their receptors (BMPR1A, BMPR1B and BMPR2). This binding can be facilitated by crossveinless 2 (CV2) (Zhang et al., 2010) or other receptor complex proteins. Once phosphorylated pSMAD1/5/8 binds SMAD4 and translocates to the nucleus where the complex acts as a transcription factor (Massague et al., 2005; Miyazono et al., 2005). In the extracellular space, availability of BMPs for binding to their receptors is regulated by the secreted proteins Chordin (CHRD), Chordin-like 1 (CHRDL1), Chordin-like 2 (CHRDL2), Noggin (NOG) and TWSG1 among others (Balemans and Van Hul, 2002). While CHRD and NOG are antagonists of BMP action, TWSG1 has a dual role, acting as either a BMP antagonist or as an agonist (Oelgeschlager et al., 2000; Ross et al., 2001) which has been shown in *Danio rerio*, *Drosophila* and *Xenopus* (Little and Mullins, 2004; Oelgeschlager et al., 2000; Shimmi et al., 2005). CHRD can be cleaved by the matrix metalloproteinase (MMP) BMP1, also known as tolloid, which can release ligand into the extracellular space. Cleavage of Chordin by BMP1 is enhanced when TWSG1 participates in the complex of Chordin and BMP (Xie and Fisher, 2005).

Mice deficient for TWSG1 have a number of developmental defects, including craniofacial malformations (Billington et al., 2011b; MacKenzie et al., 2009; Zakin and De Robertis, 2004), defects of the vertebrae, kidneys, thymus (Nosaka et al., 2003), and other organs that require branching morphogenesis such as salivary glands (Melnick et al., 2006). Given the role of TWSG1 in the development of branched organs, the goal of this study was to understand the role of TWSG1 during postnatal ductal maturation in the MG and to determine how perturbations in BMP signaling may affect that maturation.

Materials and Methods

Mice

Generation and genotyping of mice deficient for TWSG1 (C57BL/6 background) and heterozygous gene targeted *Twsg1*/Lac-Z knock-in mice have been previously reported (Gazzerro et al., 2006; Petryk et al., 2004). Use and care of the mice in this study were approved by the University of Minnesota Institutional Animal Care and Use Committee.

Whole mount hematoxylin and X-Gal staining, elongation and branching analysis

Inguinal MGs (#4) were harvested from female mice in early puberty (Nelson et al., 1990) (day of vaginal opening, about six weeks of age). Some mice were allowed to recover and the contralateral MG was harvested at 10 weeks and stained as previously described (Li et al., 2002). MGs from 3 week old females were also collected. Mammary glands that were collected from 10 week animals were staged for metestrus by vaginal observation and vaginal smears. Briefly, whole glands were fixed in 4% paraformaldehyde (Polysciences, Inc. Warrington, PA) for 2 hours on ice, defatted with acetone and stained with hematoxylin (Fischer Scientific, Waltham, MA) cleared with xylenes and the gland flattened between two slides for image capture. For whole-mount lacZ staining, fat pads containing the mammary glands were isolated, fixed in ice-cold 2% formaldehyde, 0.2% gluteraldehyde, 0.01% sodium deoxycholate, 0.02% Nonidet-P40 (NP40) in PBS for 5 min, washed with 2mM $MgCl_2$ in PBS, and stained overnight in X-gal solution [0.1 M phosphate pH 7.3, 2 mM $MgCl_2$, 0.01 % sodium deoxycholate, 0.02 % NP40, 5 mM $K_3Fe(CN)_6$, 5 mM $K_4Fe(CN)_6$]

supplemented with 1 mg X-Gal (Promega) on a rotating wheel at room temperature in the dark overnight. Following washing in PBS and refixing in 2% formaldehyde, 0.2% gluteraldehyde, the pads where photographed or dehydrated and processed for paraffin embedding and sectioning. The extent of fat pad colonization, secondary branching and TEB area were calculated as previously described (Khialeeva et al., 2011; McCaffrey and Macara, 2009; Richards et al., 2004). Briefly, the length and width of the ductal tree were measured as well as the length and width of the stromal fat pad. Areas were calculated for both, and a ductal tree: fat pad ratio was calculated. The extent of secondary branching was calculated by counting branch points within a 2 × 3-mm^2 area within 1mm of the lymph node and TEB area was calculated by using the freehand tool in ImageJ (Rasband, 1997–2011) to trace the TEB, diameter was also calculated using the straight line tool.

Immunohistochemistry

Female mice at the onset of puberty were injected intraperitoneally (30 ng/g bodyweight) with bromo-2′-deoxy-uridine (BrdU) (Roche, Indianapolis, IN) and sacrificed 3 hours later. Inguinal MGs (#4) were harvested and fixed in 4% paraformaldehyde on ice for 2 hours, embedded in paraffin and sectioned at 5μM. Sections were deparaffinized in xylenes, rehydrated through a series of graded ethanols. For pSMAD1/5/8, GATA-3, ECAD, K8 and K14 staining, antigen retrieval was performed. Slides were placed in Antigen Unmasking Solution diluted to manufacturer's recommendation (Vector Laboratories, Burlington, CA) and microwaved for 20 minutes. Once cooled, slides were washed and then blocked in PBS containing 5% goat serum (Invitrogen, Carlsbad, CA) and 0.3% Triton X-100 (Fisher Scientific) for 60 minutes at room temperature. Sections were incubated with anti-pSMAD1/5/8 (Cell Signaling Technology Inc., Danvers, MA) 1:50, anti-GATA-3 (BD Pharmigen, San Diego, CA) 1:50, anti-E-Cadherin (Cell Signaling Technology Inc.) 1:100, anti-Keratin-14 (Covance, Princeton, NJ) 1:200, anti-Keratin-18 (TROMA-I) (Developmental Studies Hybridoma Bank, Iowa City, IA) 1:200 or anti-Progesterone receptor (Sigma) 1:50. Sections were developed either with Alexa Fluor (Invitrogen) or DyLight (AbCam, San Francisco, CA) species-appropriate fluorophore conjugated secondary antibodies. Fluorescence was visualized on a Zeiss 710 LSM Confocal Microscope using an Argon12 laser (excitation 488 nm), a HeNe laser (excitation 543 nm) a HeNe laser (excitation 633). Images were taken under identical conditions and post-acquisition manipulations were also identical.

Cell Culture

HC11 mouse mammary cells (Danielson et al., 1984) (a gift from Dr. Schwertfeger), derived from pregnant BALB/c mouse MG were cultured in RPMI 1640 medium (ATCC, Manassas, VA) supplemented with 10% fetal calf serum (ATCC), 53g/ml insulin (Sigma) and 10 ng/ml epidermal growth factor (Invitrogen). Cells were cultured in a humidified atmosphere of 5% CO2 in air at 37°C. Prior to BMP treatment cells were serum starved for 24 hours, and then treated with either BSA or recombinant BMP7 50ng/ml (R&D Systems).

Cell Proliferation and Apoptosis

BrdU incorporation was visualized using Bromo-2′-deoxy-uridine Labeling and Detection Kit II (Roche) following manufacturer's instruction and double stained with anti-K18 (Developmental Studies Hybridoma Bank) 1:200. Five TEBs per section (n=5) from 5 MGs were image captured. The number of BrdU positive cells and the total number of K18 positive cells were counted by 2 independent scorers who were blinded to genotype and the total number of BrdU positive cells are presented as a fraction of total nuclei. Using the same method, apoptotic cells were visualized with TUNEL staining (Gavrieli et al., 1992) using a DeadEnd Fluorometric TUNEL System (Promega, Madison, WI) following

manufacturer's instructions. The total number of TUNEL positive nuclei within a TEB structure was expressed as a percentage of all nuclei within that structure.

cDNA generation, RT-PCR and qRT-PCR

Whole inguinal MGs (#4) were collected from WT and *Twsg1*$^{-/-}$ virgin female mice at the onset of puberty, lymph node removed, and MG lysed in TRIzol reagent (Invitrogen). Furthermore, inguinal MGs were collected and lysed in TRIzol from WT mice at 3 weeks, 10 weeks and early pregnancy (10.5 days past coitus). After extraction with TRIzol, RNA was isolated using RNeasy micro kit (Qiagen, Germantown, MD) following manufacturer's instructions. A similar procedure was followed to obtain total RNA from HC11 cells. Reverse transcription was carried out with the Thermoscript RT-PCR System (Invitrogen) priming with Oligo $(dT)_{20}$, followed by RT and qRT- PCR (Q-PCR, MX3000p, Agilent, LaJolla, CA) for BMP pathway components. Primers for BMP pathway components have been previously published (Sun et al., 2010). Our approach, given the expected reduced epithelium within the *Twsg1*$^{-/-}$ gland, was to first calculate a ratio between *Gapdh* and *K18* and then use this ratio to normalize the signal of the gene of interest. This allowed us to look both at relative whole gland expression as well as relative epithelial expression.

Western blotting

Whole inguinal MGs were collected from virgin, female mice at the onset of puberty, lymph node removed and lysed in modified RIPA buffer (250ul of 140mM NaCl, 0.4 mM TrisHCl pH 8.0, 1% Glycerol, 1% NP40, 2% BSA with Complete Protease Inhibitor Cocktail (Roche) and PhosSTOP (Roche). SDS-PAGE was used to separate proteins and separated proteins were transferred to PVDF membrane. The membrane (Invitrogen) was blocked with Odyssey blocking buffer (LI-COR, Lincoln, NE, USA) containing 0.1% v/v Tween 20. Membranes were incubated overnight at 4°C with anti-p-Smad1/5/8 (Cell Signaling Technology Inc.) 1:250, anti-Total SMAD (Santa Cruz Biotechnology, Santa Cruz, CA) 1:100 and anti-GAPDH (ABCam, Cambridge, MA) 1:5000 antibodies and washed before incubation with species-appropriate fluorescent conjugated secondary antibodies for 1 h at room temperature. After washing to remove trace detergent, membranes were analyzed using an Odyssey Infrared Imaging System (LI-COR; Millennium Science, Surrey Hills, Australia) using the manufacturer's protocol. Relative pSMAD1/5/8 was calculated by first normalizing the signal intensity for total SMAD to GAPDH to control for loading. Then pSMAD1/5/8 signal was expressed as a percentage of the total SMAD pool. To detect GATA-3 membranes were incubated overnight at 4°C with anti- GATA-3 antibody at 1:50 dilution (AbCam, San Francisco, CA), probed with anti-mouse HRP- conjugated secondary antibody (Cell Signaling Technology Inc.), and visualized with SuperSignal West Pico Chemiluminescent Substrate (Thermo Scientific, Rockford, IL).

Mammary gland transplantation

Mammary glands from 3 week old *Twsg1*$^{-/-}$ host females or WT host females were cleared of endogenous epithelium as described (DeOme et al., 1959). Donor mammary tissue was collected from adult wild type (WT) and *Twsg1*$^{-/-}$ mice and minced into small fragments. WT and *Twsg1*$^{-/-}$ mammary fragments were transplanted into the clear host fat pads, with each host (both WT and *Twsg1*$^{-/-}$) mouse receiving a WT transplant and a contralateral *Twsg1*$^{-/-}$ transplant. Host fat pads containing transplanted epithelium were removed and processed for whole-mount hematoxylin staining as described above. Approximately 80% of all transplants were able to colonize and elongate into the host fat pad.

Statistical analyses

Gene expression levels were normalized to K18/GAPDH and significance calculated using a Student's t-test with significance set at $p < 0.05$. pSMAD signal intensity was normalized to total SMAD which was first normalized to GAPDH. Significance was calculated using a Student's t-test with significance set at $p < 0.05$.

Results

TWSG1 and other BMP signaling pathway components are present in the mammary gland during postnatal development

To determine the presence and timing of TWSG1 expression during MG postnatal development, LacZ staining of mammary glands from heterozygous mice with LacZ inserted into the *Twsg1* locus and RT-PCR for BMP pathway components was performed. *Twsg1* was detected by LacZ staining in the myoepithelium and in a subset of body cells within the canalizing TEB (Fig. 1. A,B) at 6 weeks. In the mature gland, *Twsg1* was expressed throughout the ductal tree and was primarily expressed in the myoepithelium (Fig. 1. C,D). Given that TWSG1 modulates BMP signaling, components of the BMP pathway were assessed by RT-PCR across developmentally relevant time points (Fig. 1E). mRNA for *Bmp1*, *Bmp2, Bmp6*, *Bmp7*, *Bmpr1a, Bmpr2*, and *Smad4* were expressed across all time points. The Type1 receptor *Bmpr1b* was barely detectable. *Bmp4* was detected at 10 weeks and at pregnancy. Among genes encoding BMP-binding proteins, *Twsg1* mRNA was expressed at all time points while others were more temporally expressed. *Chordin* (*Chrd)* was undetectable at 6 weeks and barely detectable at other stages, while *Chordin-like 1* (*Chrdl1*) was strongly expressed at each time point. *Noggin* (*Nog)* was expressed only during pregnancy while *Chordin-like 2 (Chrdl2)* was undetectable (Fig. S1). *Cv2* mRNA was not detected during pregnancy, but was present at other time points.

TWSG1 is required for timely ductal elongation and fat pad colonization

MGs from WT and $Twsg1^{-/-}$ female mice were examined at 3, 6 and 10 weeks. The ductal trees were comparable at 3 weeks with the establishment of a rudimentary tree (Fig. 2A,D) although TEBs appeared atypical in the $Twsg1^{-/-}$ MG (Fig. 2G). At 3 weeks, TEBs were smaller than WT and in some cases it appeared as if TEBs were not established. At 6 weeks, the WT ducts had elongated well past the lymph node (LN) while the $Twsg1^{-/-}$ ducts showed little elongation. In most cases, the ducts did not reach or just reached the LN (Fig. 2B,E). The TEBs in the $Twsg1^{-/-}$ were larger than WT TEBs at this time point (Fig. 2H). At 10 weeks, the WT ducts had completely elongated, were well branched and the TEBs had reabsorbed. In $Twsg1^{-/-}$ ducts, TEBs were still present and the ductal tree was not as robustly branched (Fig. 2C,F). At 10 weeks, the WT TEBs had reabsorbed while TEBs were still found in the $Twsg1^{-/-}$ MG (Fig. 2I). A reduction in secondary branching in $Twsg1^{-/-}$ MGs at 10 weeks was also observed. The most striking difference between WT and $Twsg1^{-/-}$ ductal morphogenesis was found at 6 weeks and this stage was assessed further.

TWSG1 is required for timely elongation and fat pad colonization

MGs from $Twsg1^{-/-}$ female mice were examined on the first day of vaginal opening, approximately 6 weeks of age. MGs from WT animals contained ducts that extended past the lymph node and were robustly branched. In contrast, $Twsg1^{-/-}$ mice showed a significant decrease in fat pad colonization (Fig. 3A) with 38% of fat pad being occupied by the ductal network in $Twsg1^{-/-}$ MGs (n=5) compared to 64% in WT MGs (n=5, p=0.0032) at 6 weeks of age. In addition, secondary branching was significantly reduced in MGs from 6 week old virgin $Twsg1^{-/-}$ animals compared to WT (Fig. 3B) and TEBs were significantly larger in $Twsg1^{-/-}$ ducts (Fig. 3C).

Delay in elongation is intrinsic to the MG

To determine if the delay in ductal elongation and fat pad colonization was intrinsic to the MG rather than secondary to other factors, for example alterations in hormonal milieu, we performed transplantation experiments. We transplanted *Twsg1*$^{-/-}$ epithelium into the fat pads, cleared of endogenous epithelium, of 3 week old WT animals. The MGs were analyzed 3 weeks later and there was either a significant delay (n=2) or no measurable outgrowth (n=1) of *Twsg1*$^{-/-}$ MG tissue when compared to contralaterally transplanted WT tissue (Fig. 4A,B). Conversely, WT MG tissue transplanted into the cleared fat pad of *Twsg1*$^{-/-}$ had outgrowth that was similar to WT tissue transplanted into WT fat pad (data not shown). The TEBs in the *Twsg1*$^{-/-}$ transplanted tissue were similar in morphology to TEBs in 3 week *Twsg1*$^{-/-}$ MGs (Fig. 4C,D).

BMP signaling is reduced in the MG epithelium

To further investigate BMP signaling within the *Twsg1*$^{-/-}$ MG, a western blot was performed to detect pSMAD1/5/8. BMP signaling via pSMAD was significantly reduced in the *Twsg1*$^{-/-}$ MG (Fig. 5A). Co-localization studies demonstrated that in the WT MG pSMAD1/5/8 was localized to nuclei of cells within the TEB and pSMAD1/5/8 signal could not be detected in the *Twsg1*$^{-/-}$ TEB (Fig. 5B). We also observed that BMP downstream targets, *Msx1*, *Msx2* and *Gata-3*, were downregulated in *Twsg1*$^{-/-}$ MG (Fig. 5C).

TWSG1 mediates lumen formation and luminal identity

Whole mount light microscopy of *Twsg1*$^{-/-}$ MGs showed a density of staining in the duct that was suggestive of a difference in cell density between WT and *Twsg1*$^{-/-}$ MGs. To investigate this further we sectioned MGs from 6 week old virgin females and stained with K18, K14 and Trichrome and assessed mature ducts. WT MGs at 6 weeks had mature ducts with a clear, well-defined lumen (Fig. 6A–C, G–I, M–N) with no cells visible within the lumen. Conversely, the *Twsg1*$^{-/-}$ MGs contained a mix of ducts containing cell islets (Fig. 6D–F), completely occluded ducts (Fig. 6J–L) as well as single cells shed into the lumen (Fig. 6Q–R) and clear lumens. Approximately 60% of the mature ducts in the *Twsg1*$^{-/-}$ MG had either complete or partial occlusion. When occluded ducts were stained for K14, the cells within the lumens contained an organized structure that consisted of a secondary K14 positive compartment surrounding a mass of K14 negative cells (Fig. 6D–F). This “duct within a duct” structure was only observed in *Twsg1*$^{-/-}$ MGs. WT, mature ducts consisted of a clearly defined luminal compartment that was K18 positive (Fig. 6G–I). Using a blood vessel landmark, the luminal compartments of *Twsg1*$^{-/-}$ ducts were further examined. In many cases, the duct remained occluded until out of the plane of sectioning and not all cells within the occlusion were K18 positive (arrows) (Fig. 6J–L). To look more closely at *Twsg1*$^{-/-}$ myoepithelial compartment, K14 stained sections were interrogated for the presence of basal body cells, which are K14 positive cells within the luminal compartment. In WT ducts, no basal body cells were observed (Fig. 6M–N), consistent with previous reports (Mailleux et al., 2007). Within *Twsg1*$^{-/-}$ MGs ~60% of the ducts observed contained K14 positive basal body cells. To further characterize the cells within the luminal compartment ducts were stained for smooth muscle actin (SMA) and a similar distribution of SMA positive cells were seen in the *Twsg1*$^{-/-}$ MG (data not shown). Additionally, we observed cell shedding in *Twsg1*$^{-/-}$ but not WT mature ducts. Usually these were single or small groups of cells within the lumens of mature ducts and these shed cells were K14 positive (Fig. 6Q,R).

Apoptotic defect may lead to accumulation of cells and poor lumen formation in *Twsg1* mutant ducts

The TEBs of MGs from *Twsg1*$^{-/-}$ animals are larger than WT controls suggesting hyperplasia. To assess this further we counted the number of cells within TEB structures (5 animals, 5 sections per animal) in WT and *Twsg1*$^{-/-}$ MGs. There was a significant increase in the number of K18 positive cells within the *Twsg1*$^{-/-}$ TEBs (Fig. 7A). To determine if this was due to an increase in proliferation or a decrease in apoptosis we stained for BrdU and performed a TUNEL assay. BrdU incorporation revealed no significant difference in proliferation between WT and *Twsg1*$^{-/-}$ TEBs (Fig. 7B,D). To determine if known regulators of proliferation are changed in our model, we assessed the expression of *insulin-like growth factor 1, amphiregulin* and *estrogen receptor alpha* by Q-PCR. There were no significant differences detected (data not shown). Furthermore, amphiregulin and progesterone receptor were visualized by IF and no differences in distribution were observed (data not shown). However, there was a marked decrease of nearly four-fold in apoptosis within the *Twsg1*$^{-/-}$ TEBs (Fig. 7C,D).

TWSG1 plays a role in restricting K14 positive cells to the basal compartment

Gata-3 is required for luminal identity in the MG and is a downstream target of BMP signaling in various tissues (Bonilla-Claudio et al., 2012). In WT TEBs (Fig. 8A–D) and mature ducts (Fig. 8I–L) almost all luminal cells expressed GATA-3. In contrast, *Twsg1*$^{-/-}$ MGs consisted of TEBs (Fig. 8E–H) and mature ducts (Fig. 8M–P) that were a mosaic of GATA-3 positive and GATA-3 negative cells. In *Twsg1*$^{-/-}$ MGs, single cells that were shed into the lumen were GATA-3 negative (Fig. 8P). To confirm that BMPs could induce *Gata-3* expression in mammary epithelial cells, HC11 cells were treated with BMP7 50ng/ml and *Gata-3* mRNA expression measured by Q-PCR. BMP7 induced *Gata-3* expression over 2-fold ($p = 0.0004$) (Fig. 9A). We also assessed *Gata-3* expression and protein content and found that *Gata-3* expression (Fig. 9B) as well as protein level (Fig. 9C) were reduced in *Twsg1*$^{-/-}$ MGs.

Discussion

TWSG1 as a positive regulator of BMP signaling during postnatal MG development

Studies in *Drosophila melanogaster*, *Danio rerio*, *Xenopus*, and *Mus musculus* have shown that TWSG1 is a highly conserved extracellular modulator of BMP signaling with important roles during embryonic development (Ross et al., 2001; Scott et al., 2001; Zusman and Wieschaus, 1985). Recent studies have demonstrated that TWSG1 continues to be an important BMP regulator in adult mammalian tissues, including bone homeostasis (Sotillo Rodriguez et al., 2009), regeneration following ischemic kidney injury (Larman et al., 2009), immune responses (Tsalavos et al., 2011), and, as this study shows, postnatal MG ductal maturation.

It is known that TWSG1 interacts with BMP2, BMP4, and BMP7 (Billington et al., 2011a; Blitz et al., 2003; Chang et al., 2001; Ross et al., 2001; Scott et al., 2001), either directly or by forming complexes with CHRD (Larrain et al., 2001). While in *Xenopus* and *Denio rario* TWSG1 can act as a BMP antagonist as well as an agonist (Blitz et al., 2003; Ross et al., 2001; Xie and Fisher, 2005), the latter function has not been directly demonstrated in mammals. In this study, BMP signaling is reduced in the murine MG in the absence of TWSG1, suggesting pro-BMP activity in the postnatal MG. It is thought that the pro-BMP activity of TWSG1 results from its ability to facilitate the cleavage of CHRD by the MMP BMP1 in the extracellular space (Larrain et al., 2001). *Chrd* was not detected in the MG at 6 weeks, suggesting that CHRD-independent mechanisms may play a role (Xie and Fisher, 2005) A potential binding partner is CHRDL1, which is highly expressed in the developing

MG and has been shown to bind BMPs and TWSG1. Intriguingly, in cells of the proximal tubule of the kidney, CHRDL1 amplifies BMP4 signaling in the presence of TWSG1 (Larman et al., 2009).

Reduced expression of the BMP targets *Msx1*, *Msx2*, *Gata-3,* and decreased levels of pSMAD1/5/8 all indicate a reduction of BMP signaling in the *Twsg1*$^{-/-}$ MG. Mutations in *Msx1* and *Msx2* result in impaired MG development. MGs of *Msx2*-deficient mice arrest at the mammary sprout stage while the epithelium of the *Msx1/Msx2* double-deficient mice fails to form a bud with subsequent regression of the MG anlagen (Satokata et al., 2000). *Bmp2* and *Bmp4* mutants are embryonic lethal (Lawson et al., 1999; Zhang and Bradley, 1996) and no studies have specifically addressed the effects of deletion of these genes in the postnatal MG. Thus, the *Twsg1*$^{-/-}$ mouse provides a model in which to evaluate the consequences of perturbated BMP signaling during postnatal ductal maturation.

TWSG1 is essential for postnatal ductal maturation in the murine MG

Postnatal MG development is orchestrated by numerous hormones, growth factors, cytokines, and transcription factors including MSX1, MSX2 and GATA-3, which regulate proliferation, apoptosis, and differentiation (McNally and Martin, 2011). Although BMPs are known to regulate proliferation through *Msx1* (Zhang et al., 2002) and the expression of *Msx1* was decreased in the *Twsg1*$^{-/-}$ MG, proliferation was not significantly altered suggesting that other pathways are involved in regulating proliferation in the elongating duct. In contrast, apoptosis was reduced in *Twsg1*$^{-/-}$ MG, indicating a role for BMP-induced apoptosis in lumen formation. Furthermore, *Twsg1* is expressed in a subset of body cells within the TEB making it available for regulation of BMP signaling within the canalizing TEB. The classical mediator of the pro-apoptotic effects of BMPs is *Msx2* (Graham et al., 1996). Indeed, reduced *Msx2* expression was seen in the *Twsg1*$^{-/-}$ MG. The reduced apoptosis in the TEB could explain the observation that 60% of the mature ducts in the *Twsg1*$^{-/-}$ MG were occluded or had cell islets present in the lumen. It has been shown that disrupted apoptosis can be accompanied by lumen filling and cell shedding in the MG (Mailleux et al., 2007). However, it is also possible that cells shed into the lumen repopulate the lumen with a mass of cells that is later cleared by some unknown mechanism.

GATA-3 is directly induced by BMP signaling during facial skeletal development (Bonilla-Claudio et al., 2012), preplacodal ectoderm specification (Kwon et al., 2010), and hair follicle morphogenesis (Kobielak et al., 2003). In the MG, GATA-3 deficiency results in impaired placode formation, elongation defect as a result of the failure of TEBs to stably form, and a reduction in side branching (Asselin-Labat et al., 2007). Additionally, GATA-3 can induce apoptosis in a luminal tumor model (Kouros-Mehr et al., 2008) and upregulate pro-apoptotic genes such as *caspase-14* (Asselin-Labat et al., 2011). In mice with MG specific GATA-3 deficiency lumens are irregular and cell shedding is observed (Asselin-Labat et al., 2007). In the *Twsg1*$^{-/-}$ MG, loss of TWSG1 reduces BMP signaling perhaps by reducing BMP availability. As a result, not all cells reach the BMP signaling threshold required for *Gata-3* induction and subsequent adoption of a luminal cell fate. The cells that fail to induce *Gata-3* will remain in the luminal compartment or be shed into the lumen. It is possible that this mosaic of cell types in the advancing duct inhibits elongation but as cells are lost into the lumen cell:cell contacts are reestablished and elongation can again proceed in the absence of Twsg1$^{-/-}$.

We also observed a decrease in secondary branching in *Twsg1*$^{-/-}$ MG. As the ducts invade into the fat pad, secondary branching occurs in areas where there is low TGF3 expression (Pierce et al., 1993) and high *Msx2* expression (Satoh et al., 2004). A recent study demonstrated that BMP2/4 can induce branching in the MG via *Msx2* upregulation (Fleming et al.). When *Twsg1* is deleted, some cells receive adequate BMP while others do not and in

those regions with reduced BMP, *Msx2* expression is also reduced and branching is not initiated, thus leading to an overall reduction in secondary branching in the *Twsg1*$^{-/-}$ MG.

Contribution of TWSG1 to maintaining basal vs luminal epithelial identity

The MG epithelium is composed of the basal myoepithelial cells and polarized luminal epithelial cells. It is thought that the different cell populations arise from multipotent progenitors, or mammary stem cells (Stingl et al., 1998). Interestingly, in *Twsg1*$^{-/-}$ MG, K14 positive cells are present within the luminal compartment among K18 positive cells. This suggests that BMP signaling plays a role in establishing and/or maintaining epithelial identity as opposed to myoepithelial, for example through GATA-3 (Metallo et al., 2008; Wilson and Hemmati-Brivanlou, 1995). In *Twsg1*$^{-/-}$ MGs, the K14 positive cells within the luminal compartment may represent those cells whose BMP exposure was not sufficient to induce *Gata-3* expression preventing progression towards a terminal luminal fate. In line with this, cells shed into the lumen of *Twsg1*$^{-/-}$ MGs are K14 positive whereas a previous study demonstrated that deleting *Gata-3* after luminal specification did not reduce K18 expression showing that GATA-3 is not required for maintenance of K18, only its induction (Kouros-Mehr et al., 2006). This suggests that TWSG1 acts upstream of GATA-3 for regulating epithelial/myoepithelial cell fate.

In summary, this study sheds light on the role of the extracellular regulation of BMP signaling by TWSG1 during postnatal MG development. It shows that BMP signaling is reduced in MG leading to a decrease in *Msx2* and *Gata-3* expression. In the absence of TWSG1, delayed ductal elongation, impaired branching and lumen formation, incomplete myoepithelial restriction, and shedding into the lumen are observed. Understanding how TWSG1 regulates normal ductal maturation can provide insight into what role it may be playing during carcinogenesis, especially in light of the recent data suggesting tumor suppressor effects of BMPs (Loh et al., 2008; Owens et al., 2012; Ye et al., 2009). There is some evidence that the expression of *Bmps*, *Msx2*, and *Twsg1* is altered in breast cancer (Finak et al., 2008; Malewski et al., 2005; Phippard et al., 1996), but the mechanisms for this differential regulation are unknown. Future studies will further elucidate the mechanism by which the lumens are eventually cleared in the absence of TWSG1. This may provide insight into how cells within the MG that escape targeted apoptosis at one point in development are identified and eventually cleared from the MG.

Supplementary Material

Refer to Web version on PubMed Central for supplementary material.

Acknowledgments

The authors thank Brian Schmidt, T.J. Beadnell and Johanna Reed for technical assistance. We also thank Charles Billington Jr. for assistance with graphics, statistical analyses and helpful conversations. This project was supported by Department of Defense Breast Cancer Research Predoctoral Fellowship BC100263 to C.L.F., R01 DE016601 to A.P., Minnesota Medical Foundation #4064-9201-11 to A.P., Viking Children's Fund grant-in-aid of research to A.P., and Undergraduate Research Opportunities Program (UROP) to B.C.N and R.K.H.; C.K. was supported by the University of Minnesota's School of Dentistry Summer Research Fellowship.

References

Asselin-Labat M-L, Sutherland KD, Vaillant F, Gyorki DE, Wu D, Holroyd S, Breslin K, Ward T, Shi W, Bath ML, Deb S, Fox SB, Smyth GK, Lindeman GJ, Visvader JE. Gata-3 negatively regulates the tumor-initiating capacity of mammary luminal progenitor cells and targets the putative tumor suppressor caspase-14. Mol Cell Biol. 2011 MCB.05766–11.

Asselin-Labat ML, Sutherland KD, Barker H, Thomas R, Shackleton M, Forrest NC, Hartley L, Robb L, Grosveld FG, van der Wees J, Lindeman GJ, Visvader JE. Gata-3 is an essential regulator of mammary-gland morphogenesis and luminal-cell differentiation. Nat Cell Biol. 2007; 9:201–9. [PubMed: 17187062]

Bailey JM, Singh PK, Hollingsworth MA. Cancer metastasis facilitated by developmental pathways: Sonic hedgehog, Notch, and bone morphogenic proteins. J Cell Biochem. 2007; 102:829–39. [PubMed: 17914743]

Balemans W, Van Hul W. Extracellular regulation of BMP signaling in vertebrates: a cocktail of modulators. Dev Biol. 2002; 250:231–50. [PubMed: 12376100]

Beppu H, Mwizerwa ON, Beppu Y, Dattwyler MP, Lauwers GY, Bloch KD, Goldstein AM. Stromal inactivation of BMPRII leads to colorectal epithelial overgrowth and polyp formation. Oncogene. 2008; 27:1063–70. [PubMed: 17700526]

Billington CJ Jr, Fiebig JE, Forsman CL, Pham L, Burbach N, Sun M, Jaskoll T, Mansky K, Gopalakrishnan R, O'Connor MB, Mueller TD, Petryk A. Glycosylation of Twisted Gastrulation is Required for BMP Binding and Activity during Craniofacial Development. Front Physiol. 2011a; 2:59. [PubMed: 21941513]

Billington CJ Jr, Ng B, Forsman C, Schmidt B, Bagchi A, Symer DE, Schotta G, Gopalakrishnan R, Sarver AL, Petryk A. The molecular and cellular basis of variable craniofacial phenotypes and their genetic rescue in Twisted gastrulation mutant mice. Dev Biol. 2011b; 355:21–31. [PubMed: 21549111]

Blitz IL, Cho KW, Chang C. Twisted gastrulation loss-of-function analyses support its role as a BMP inhibitor during early Xenopus embryogenesis. Development. 2003; 130:4975–88. [PubMed: 12952901]

Bonilla-Claudio M, Wang J, Bai Y, Klysik E, Selever J, Martin JF. Bmp signaling regulates a dose-dependent transcriptional program to control facial skeletal development. Development. 2012; 139:709–719. [PubMed: 22219353]

Bowman A, Nusse R. Location, Location, Location: FoxM1 Mediates β-Catenin Nuclear Translocation and Promotes Glioma Tumorigenesis. Cancer Cell. 2011; 20:415–416. [PubMed: 22014565]

Buijs JT, van der Horst G, van den Hoogen C, Cheung H, de Rooij B, Kroon J, Petersen M, van Overveld PGM, Pelger RCM, van der Pluijm G. The BMP2/7 heterodimer inhibits the human breast cancer stem cell subpopulation and bone metastases formation. Oncogene. 2012; 31:2164–74. [PubMed: 21996751]

Chang C, Holtzman DA, Chau S, Chickering T, Woolf EA, Holmgren LM, Bodorova J, Gearing DP, Holmes WE, Brivanlou AH. Twisted gastrulation can function as a BMP antagonist. Nature. 2001; 410:483–7. [PubMed: 11260717]

Cho KW, Kim JY, Song SJ, Farrell E, Eblaghie MC, Kim HJ, Tickle C, Jung HS. Molecular interactions between Tbx3 and Bmp4 and a model for dorsoventral positioning of mammary gland development. Proc Natl Acad Sci U S A. 2006; 103:16788–93. [PubMed: 17071745]

Danielson KG, Oborn CJ, Durban EM, Butel JS, Medina D. Epithelial mouse mammary cell line exhibiting normal morphogenesis in vivo and functional differentiation in vitro. Proc Natl Acad Sci U S A. 1984; 81:3756–60. [PubMed: 6587390]

DeOme KB, Faulkin LJ, Bern HA, Blair PB. Development of Mammary Tumors from Hyperplastic Alveolar Nodules Transplanted into Gland-free Mammary Fat Pads of Female C3H Mice. Cancer Research. 1959; 19:515. [PubMed: 13663040]

Dulbecco R, Henahan M, Armstrong B. Cell types and morphogenesis in the mammary gland. Proceedings of the National Academy of Sciences. 1982; 79:7346–7350.

Finak G, Bertos N, Pepin F, Sadekova S, Souleimanova M, Zhao H, Chen H, Omeroglu G, Meterissian S, Omeroglu A, Hallett M, Park M. Stromal gene expression predicts clinical outcome in breast cancer. Nat Med. 2008; 14:518–527. [PubMed: 18438415]

Fleming JM, Ginsburg E, Goldhar AS, Plant J, Vonderhaar BK. Progesterone Receptor Activates Msx2 Expression by Downregulating TNAP/Akp2 and Activating the Bmp Pathway in EpH4 Mouse Mammary Epithelial Cells. PLoS ONE. 2012; 7:e34058. [PubMed: 22457812]

Gavrieli Y, Sherman Y, Ben-Sasson SA. Identification of programmed cell death in situ via specific labeling of nuclear DNA fragmentation. The Journal of Cell Biology. 1992; 119:493–501. [PubMed: 1400587]

Gazzerro E, Deregowski V, Stadmeyer L, Gale NW, Economides AN, Canalis E. Twisted gastrulation, a bone morphogenetic protein agonist/antagonist, is not required for post-natal skeletal function. Bone. 2006; 39:1252–1260. [PubMed: 16934545]

Graham A, Koentges G, Lumsden A. Neural Crest Apoptosis and the Establishment of Craniofacial Pattern: An Honorable Death. Mol Cell Neurosci. 1996; 8:76–83.

Hens JR, Dann P, Zhang JP, Harris S, Robinson GW, Wysolmerski J. BMP4 and PTHrP interact to stimulate ductal outgrowth during embryonic mammary development and to inhibit hair follicle induction. Development. 2007; 134:1221–30. [PubMed: 17301089]

Hens JR, Wysolmerski JJ. Key stages of mammary gland development: molecular mechanisms involved in the formation of the embryonic mammary gland. Breast Cancer Res. 2005; 7:220–4. [PubMed: 16168142]

Hovey RC, Trott JF. Morphogenesis of mammary gland development. Adv Exp Med Biol. 2004; 554:219–28. [PubMed: 15384579]

Humphreys RC, Krajewska M, Krnacik S, Jaeger R, Weiher H, Krajewski S, Reed JC, Rosen JM. Apoptosis in the terminal endbud of the murine mammary gland: a mechanism of ductal morphogenesis. Development. 1996; 122:4013–4022. [PubMed: 9012521]

Jardé T, Dale T. Wnt signalling in murine postnatal mammary gland development. Acta Physiologica. 2012; 204:118–27. [PubMed: 21518264]

Khialeeva E, Lane TF, Carpenter EM. Disruption of reelin signaling alters mammary gland morphogenesis. Development. 2011; 138:767–776. [PubMed: 21266412]

Kobielak K, Pasolli HA, Alonso L, Polak L, Fuchs E. Defining BMP functions in the hair follicle by conditional ablation of BMP receptor IA. The Journal of Cell Biology. 2003; 163:609–623. [PubMed: 14610062]

Kouros-Mehr H, Bechis SK, Slorach EM, Littlepage LE, Egeblad M, Ewald AJ, Pai S-Y, Ho IC, Werb Z. GATA-3 Links Tumor Differentiation and Dissemination in a Luminal Breast Cancer Model. Cancer Cell. 2008; 13:141–152. [PubMed: 18242514]

Kouros-Mehr H, Slorach EM, Sternlicht MD, Werb Z. GATA-3 maintains the differentiation of the luminal cell fate in the mammary gland. Cell. 2006; 127:1041–55. [PubMed: 17129787]

Kwon H-J, Bhat N, Sweet EM, Cornell RA, Riley BB. Identification of Early Requirements for Preplacodal Ectoderm and Sensory Organ Development. PLoS Genet. 2010; 6:e1001133. [PubMed: 20885782]

Larman BW, Karolak MJ, Adams DC, Oxburgh L. Chordin-like 1 and twisted gastrulation 1 regulate BMP signaling following kidney injury. J Am Soc Nephrol. 2009; 20:1020–31. [PubMed: 19357253]

Larrain J, Oelgeschlager M, Ketpura NI, Reversade B, Zakin L, De Robertis EM. Proteolytic cleavage of Chordin as a switch for the dual activities of Twisted gastrulation in BMP signaling. Development. 2001; 128:4439–47. [PubMed: 11714670]

Lawson KA, Dunn NR, Roelen BAJ, Zeinstra LM, Davis AM, Wright CVE, Korving JPWFM, Hogan BLM. Bmp4 is required for the generation of primordial germ cells in the mouse embryo. Genes & Development. 1999; 13:424–436. [PubMed: 10049358]

Li G, Robinson GW, Lesche R, Martinez-Diaz H, Jiang Z, Rozengurt N, Wagner KU, Wu DC, Lane TF, Liu X, Hennighausen L, Wu H. Conditional loss of PTEN leads to precocious development and neoplasia in the mammary gland. Development. 2002; 129:4159–70. [PubMed: 12163417]

Little SC, Mullins MC. Twisted gastrulation promotes BMP signaling in zebrafish dorsal-ventral axial patterning. Development. 2004; 131:5825–35. [PubMed: 15525664]

Liu F, Bloch N, Bhushan KR, De Grand AM, Tanaka E, Solazzo S, Mertyna PM, Goldberg N, Frangioni JV, Lenkinski RE. Humoral bone morphogenetic protein 2 is sufficient for inducing breast cancer microcalcification. Mol Imaging. 2008; 7:175–86. [PubMed: 19123988]

Loh K, Chia JA, Greco S, Cozzi S-J, Buttenshaw RL, Bond CE, Simms LA, Pike T, Young JP, Jass JR, Spring KJ, Leggett BA, Whitehall VLJ. Bone morphogenic protein 3 inactivation is an early

and frequent event in colorectal cancer development. Genes, Chromosomes and Cancer. 2008; 47:449–460. [PubMed: 18311777]

MacKenzie B, Wolff R, Lowe N, Billington CJ Jr, Peterson A, Schmidt B, Graf D, Mina M, Gopalakrishnan R, Petryk A. Twisted gastrulation limits apoptosis in the distal region of the mandibular arch in mice. Dev Biol. 2009; 328:13–23. [PubMed: 19389368]

Mailleux AA, Overholtzer M, Schmelzle T, Bouillet P, Strasser A, Brugge JS. BIM Regulates Apoptosis during Mammary Ductal Morphogenesis, and Its Absence Reveals Alternative Cell Death Mechanisms. Developmental Cell. 2007; 12:221–234. [PubMed: 17276340]

Malewski T, Milewicz T, Krzysiek J, Gregoraszczuk EL, Augustowska K. Regulation of Msx2 gene expression by steroid hormones in human nonmalignant and malignant breast cancer explants cultured in vitro. Cancer Invest. 2005; 23:222–8. [PubMed: 15945508]

Massague J, Seoane J, Wotton D. Smad transcription factors. Genes Dev. 2005; 19:2783–810. [PubMed: 16322555]

McCaffrey LM, Macara IG. The Par3/aPKC interaction is essential for end bud remodeling and progenitor differentiation during mammary gland morphogenesis. Genes & Development. 2009; 23:1450–1460. [PubMed: 19528321]

McEvoy J, Flores-Otero J, Zhang J, Nemeth K, Brennan R, Bradley C, Krafcik F, Rodriguez-Galindo C, Wilson M, Xiong S, Lozano G, Sage J, Fu L, Louhibi L, Trimarchi J, Pani A, Smeyne R, Johnson D, Dyer Michael A. Coexpression of Normally Incompatible Developmental Pathways in Retinoblastoma Genesis. Cancer Cell. 2011; 20:260–275. [PubMed: 21840489]

McNally S, Martin F. Molecular regulators of pubertal mammary gland development. Annals of Medicine. 2011; 43:212–234. [PubMed: 21417804]

Melnick M, Petryk A, Abichaker G, Witcher D, Person AD, Jaskoll T. Embryonic salivary gland dysmorphogenesis in Twisted gastrulation deficient mice. Arch Oral Biol. 2006; 51:433–8. [PubMed: 16289463]

Metallo CM, Ji L, de Pablo JJ, Palecek SP. Retinoic Acid and Bone Morphogenetic Protein Signaling Synergize to Efficiently Direct Epithelial Differentiation of Human Embryonic Stem Cells. Stem Cells. 2008; 26:372–380. [PubMed: 17962700]

Miyazono K, Maeda S, Imamura T. BMP receptor signaling: transcriptional targets, regulation of signals, and signaling cross-talk. Cytokine Growth Factor Rev. 2005; 16:251–63. [PubMed: 15871923]

Montesano R. Bone morphogenetic protein-4 abrogates lumen formation by mammary epithelial cells and promotes invasive growth. Biochem Biophys Res Commun. 2007; 353:817–22. [PubMed: 17189614]

Nelson JF, Karelus K, Felicio LS, Johnson TE. Genetic influences on the timing of puberty in mice. Biology of Reproduction. 1990; 42:649–655. [PubMed: 2346773]

Nosaka T, Morita S, Kitamura H, Nakajima H, Shibata F, Morikawa Y, Kataoka Y, Ebihara Y, Kawashima T, Itoh T, Ozaki K, Senba E, Tsuji K, Makishima F, Yoshida N, Kitamura T. Mammalian twisted gastrulation is essential for skeleto-lymphogenesis. Mol Cell Biol. 2003; 23:2969–80. [PubMed: 12665593]

Oelgeschlager M, Larrain J, Geissert D, De Robertis EM. The evolutionarily conserved BMP-binding protein Twisted gastrulation promotes BMP signalling. Nature. 2000; 405:757–63. [PubMed: 10866189]

Owens P, Pickup MW, Novitskiy SV, Chytil A, Gorska AE, Aakre ME, West J, Moses HL. Disruption of bone morphogenetic protein receptor 2 (BMPR2) in mammary tumors promotes metastases through cell autonomous and paracrine mediators. Proceedings of the National Academy of Sciences. 2012; 109:2814–9.

Petryk A, Anderson RM, Jarcho MP, Leaf I, Carlson CS, Klingensmith J, Shawlot W, O'Connor MB. The mammalian twisted gastrulation gene functions in foregut and craniofacial development. Dev Biol. 2004; 267:374–86. [PubMed: 15013800]

Phippard DJ, Weber-Hall SJ, Sharpe PT, Naylor MS, Jayatalake H, Maas R, Woo I, Roberts-Clark D, Francis-West PH, Liu YH, Maxson R, Hill RE, Dale TC. Regulation of Msx-1, Msx-2, Bmp-2 and Bmp-4 during foetal and postnatal mammary gland development. Development. 1996; 122:2729–37. [PubMed: 8787747]

Pierce DF, Johnson MD, Matsui Y, Robinson SD, Gold LI, Purchio AF, Daniel CW, Hogan BL, Moses HL. Inhibition of mammary duct development but not alveolar outgrowth during pregnancy in transgenic mice expressing active TGF-beta 1. Genes & Development. 1993; 7:2308–2317. [PubMed: 8253379]

Rasband, WS. ImageJ. U. S. National Institutes of Health; Bethesda, Maryland, USA: 1997–2011.

Richards RG, Klotz DM, Walker MP, DiAugustine RP. Mammary Gland Branching Morphogenesis Is Diminished in Mice with a Deficiency of Insulin-like Growth Factor-I (IGF-I), But Not in Mice with a Liver-Specific Deletion of IGF-I. Endocrinology. 2004; 145:3106–3110. [PubMed: 15059953]

Ross JJ, Shimmi O, Vilmos P, Petryk A, Kim H, Gaudenz K, Hermanson S, Ekker SC, O'Connor MB, Marsh JL. Twisted gastrulation is a conserved extracellular BMP antagonist. Nature. 2001; 410:479–83. [PubMed: 11260716]

Satoh K, Ginsburg E, Vonderhaar BK. Msx-1 and Msx-2 in mammary gland development. J Mammary Gland Biol Neoplasia. 2004; 9:195–205. [PubMed: 15300013]

Satokata I, Ma L, Ohshima H, Bei M, Woo I, Nishizawa K, Maeda T, Takano Y, Uchiyama M, Heaney S, Peters H, Tang Z, Maxson R, Maas R. Msx2 deficiency in mice causes pleiotropic defects in bone growth and ectodermal organ formation. Nat Genet. 2000; 24:391–5. [PubMed: 10742104]

Schwertfeger KL. Fibroblast growth factors in development and cancer: insights from the mammary and prostate glands. Curr Drug Targets. 2009; 10:632–44. [PubMed: 19601767]

Scott IC, Blitz IL, Pappano WN, Maas SA, Cho KW, Greenspan DS. Homologues of Twisted gastrulation are extracellular cofactors in antagonism of BMP signalling. Nature. 2001; 410:475–8. [PubMed: 11260715]

Shimmi O, Umulis D, Othmer H, O'Connor MB. Facilitated Transport of a Dpp/Scw Heterodimer by Sog/Tsg Leads to Robust Patterning of the Drosophila Blastoderm Embryo. Cell. 2005; 120:873–886. [PubMed: 15797386]

Singh A, Morris RJ. The Yin and Yang of bone morphogenetic proteins in cancer. Cytokine Growth Factor Rev. 2010; 21:299–313. [PubMed: 20688557]

Sotillo Rodriguez JE, Mansky KC, Jensen ED, Carlson AE, Schwarz T, Pham L, MacKenzie B, Prasad H, Rohrer MD, Petryk A, Gopalakrishnan R. Enhanced osteoclastogenesis causes osteopenia in twisted gastrulation-deficient mice through increased BMP signaling. J Bone Miner Res. 2009; 24:1917–26. [PubMed: 19419314]

Stingl J, Emerman JT, Eaves CJ, Kuusk U. Phenotypic and functional characterization in vitro of a multipotent epithelial cell present in the normal adult human breast. Differentiation. 1998; 63:201–213. [PubMed: 9745711]

Sun M, Forsman C, Sergi C, Gopalakrishnan R, O'Connor MB, Petryk A. The expression of twisted gastrulation in postnatal mouse brain and functional implications. Neuroscience. 2010; 169:920–931. [PubMed: 20493240]

Tsalavos S, Segklia K, Passa O, Petryk A, O'Connor MB, Graf D. Involvement of twisted gastrulation in T cell-independent plasma cell production. J Immunol. 2011; 186:6860–70. [PubMed: 21572028]

van Genderen C, Okamura RM, Fariñas I, Quo RG, Parslow TG, Bruhn L, Grosschedl R. Development of several organs that require inductive epithelial-mesenchymal interactions is impaired in LEF-1-deficient mice. Genes & Development. 1994; 8:2691–2703. [PubMed: 7958926]

Virtanen S, Alarmo E-L, Sandström S, Ampuja M, Kallioniemi A. Bone morphogenetic protein -4 and -5 in pancreatic cancer–Novel bidirectional players. Experimental Cell Research. 2011; 317:2136–2146. [PubMed: 21704030]

Wagner DO, Sieber C, Bhushan R, Borgermann JH, Graf D, Knaus P. BMPs: from bone to body morphogenetic proteins. Sci Signal. 2010; 3:mr1. [PubMed: 20124549]

Wang K, Feng H, Ren W, Sun X, Luo J, Tang M, Zhou L, Weng Y, He T-C, Zhang Y. BMP9 inhibits the proliferation and invasiveness of breast cancer cells MDA-MB-231. Journal of Cancer Research and Clinical Oncology. 2011a; 137:1687–1696. [PubMed: 21892652]

Wang NJ, Sanborn Z, Arnett KL, Bayston LJ, Liao W, Proby CM, Leigh IM, Collisson EA, Gordon PB, Jakkula L, Pennypacker S, Zou Y, Sharma M, North JP, Vemula SS, Mauro TM, Neuhaus IM, LeBoit PE, Hur JS, Park K, Huh N, Kwok P-Y, Arron ST, Massion PP, Bale AE, Haussler D, Cleaver JE, Gray JW, Spellman PT, South AP, Aster JC, Blacklow SC, Cho RJ. Loss-of-function mutations in Notch receptors in cutaneous and lung squamous cell carcinoma. Proceedings of the National Academy of Sciences. 2011b; 108:17761–17766.

Watson CJ, Oliver CH, Khaled WT. Cytokine signalling in mammary gland development. Journal of Reproductive Immunology. 2011; 88:124–129. [PubMed: 21255846]

Wilson PA, Hemmati-Brivanlou A. Induction of epidermis and inhibition of neural fate by Bmp-4. Nature. 1995; 376:331–333. [PubMed: 7630398]

Xie J, Fisher S. Twisted gastrulation enhances BMP signaling through chordin dependent and independent mechanisms. Development. 2005; 132:383–91. [PubMed: 15604098]

Ye L, Kynaston H, Jiang WG. Bone morphogenetic protein-10 suppresses the growth and aggressiveness of prostate cancer cells through a Smad independent pathway. J Urol. 2009; 181:2749–59. [PubMed: 19375725]

Zakin L, De Robertis EM. Inactivation of mouse Twisted gastrulation reveals its role in promoting Bmp4 activity during forebrain development. Development. 2004; 131:413–24. [PubMed: 14681194]

Zhang H, Bradley A. Mice deficient for BMP2 are nonviable and have defects in amnion/chorion and cardiac development. Development. 1996; 122:2977–2986. [PubMed: 8898212]

Zhang J-L, Patterson LJ, Qiu L-Y, Graziussi D, Sebald W, Hammerschmidt M. Binding between Crossveinless-2 and Chordin Von Willebrand Factor Type C Domains Promotes BMP Signaling by Blocking Chordin Activity. PLoS ONE. 2010; 5:e12846. [PubMed: 20886103]

Zhang Z, Song Y, Zhao X, Zhang X, Fermin C, Chen Y. Rescue of cleft palate in Msx1-deficient mice by transgenic Bmp4 reveals a network of BMP and Shh signaling in the regulation of mammalian palatogenesis. Development. 2002; 129:4135–4146. [PubMed: 12163415]

Zusman SB, Wieschaus EF. Requirements for zygotic gene activity during gastrulation in Drosophila melanogaster. Dev Biol. 1985; 111:359–71. [PubMed: 3930314]

Highlights

- TWSG1 promotes BMP signaling in the developing mammary gland.
- TWSG1 null MGs have defects in ductal elongation, secondary branching and apoptosis.
- TWSG1 null MGs have occluded lumens and enlarged terminal end buds.
- TWSG1 null ducts fail to restrict myoepithelium to the basal layer.
- GATA-3, which is required for luminal identity, is reduced in TWSG1 null MGs.

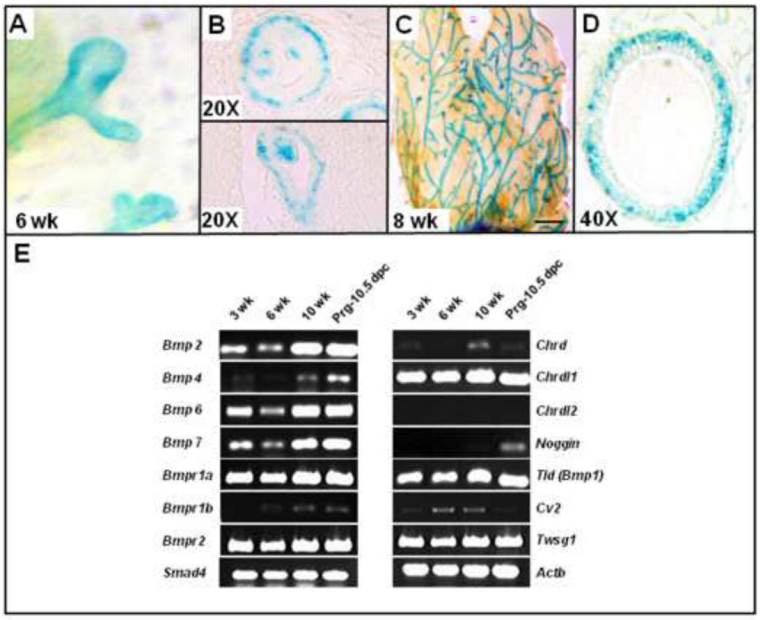

Fig. 1. *Twsg1* and BMP pathway components are expressed in the mammary gland (MG) at important postnatal developmental time points

(A–D) LacZ staining of whole mount (A,C) and sectioned (B,D) mammary glands isolated from heterozygous 6 and 8 week old virgin female carrying *LacZ* reporter gene in the *Twsg1* locus. (A) *Twsg1* is present in ducts and terminal end buds (TEBs) at 6 weeks (B) and in a subset of body cells in the canalizing TEB. (C) *Twsg1* expression is present in the mature ducts (2 mm scale bar). (D) This expression is observed primarily in the myoepithelium at 8 weeks (E) RT-PCR showing temporal expression of BMP pathway members in MGs at different postnatal developmental time points. *Actb,* beta-actin*, Chrd*, chordin; *Chrdl1*, chordin-like 1; *Chrdl2,* chordin-like 2; *Cv2,* crossveinless 2.

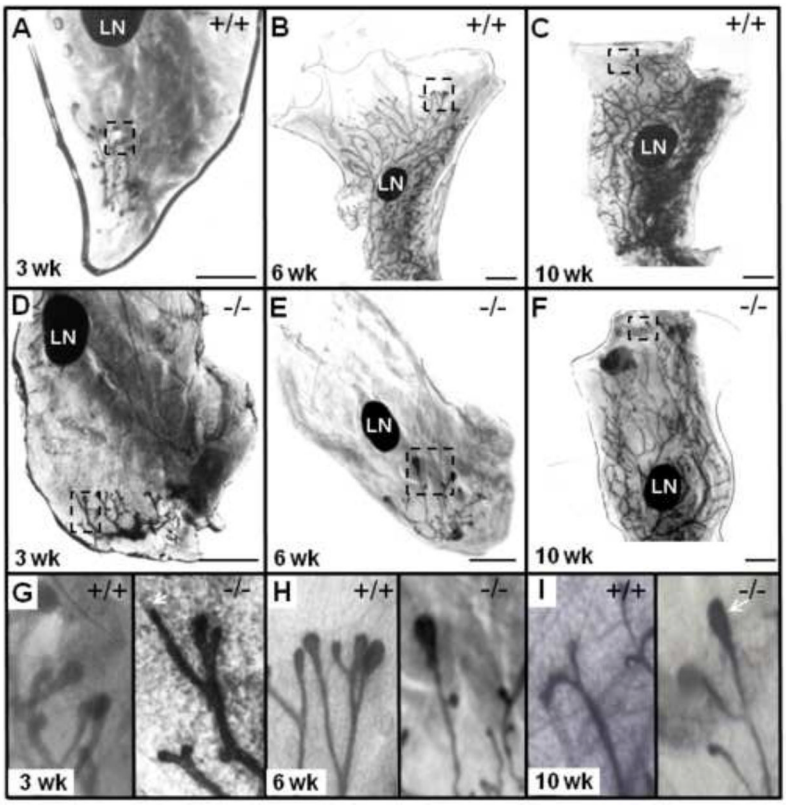

Fig. 2. Loss of TWSG1 results in a delay of ductal elongation

(A, B, C) Whole mount MG from 3 week, 6 week and 10 week old wild type (WT) virgin female mouse. **(D, E, F)** Whole mount MG from 3 week, 6 week and 10 week old *Twsg1*$^{-/-}$ virgin female mouse. **(G, H, I)** Distal ends of ductal tree from the MG of 3 week, 6 week and 10 week WT and *Twsg1*$^{-/-}$ virgin female mouse. Arrow indicates poorly formed TEB (2G) and TEBs still present at 10 weeks (2I) in the *Twsg1*$^{-/-}$ MG. Magnified distal ends are boxed. LN, lymph node. Scale bar 2 mm.

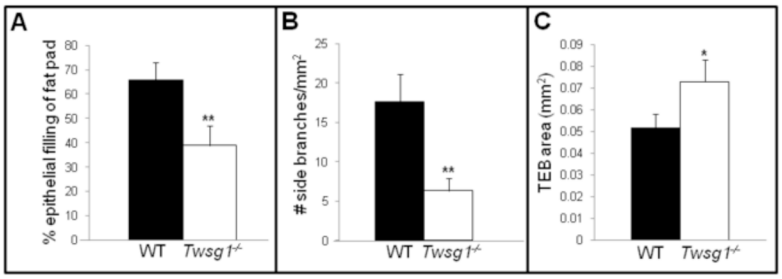

Fig. 3. Loss of TWSG1 results in impaired ductal elongation, reduced secondary branching and enlarged terminal end buds

(A) Percetage of fat pad colonization by the ductal tree in WT and *Twsg1*$^{-/-}$ virgin female mouse. **(B)** Side branching is significantly reduced in *Twsg1*$^{-/-}$ MG. **(C)** TEBs are significantly larger in *Twsg1*$^{-/-}$ MGs at 6 weeks. ** $p<0.001$,

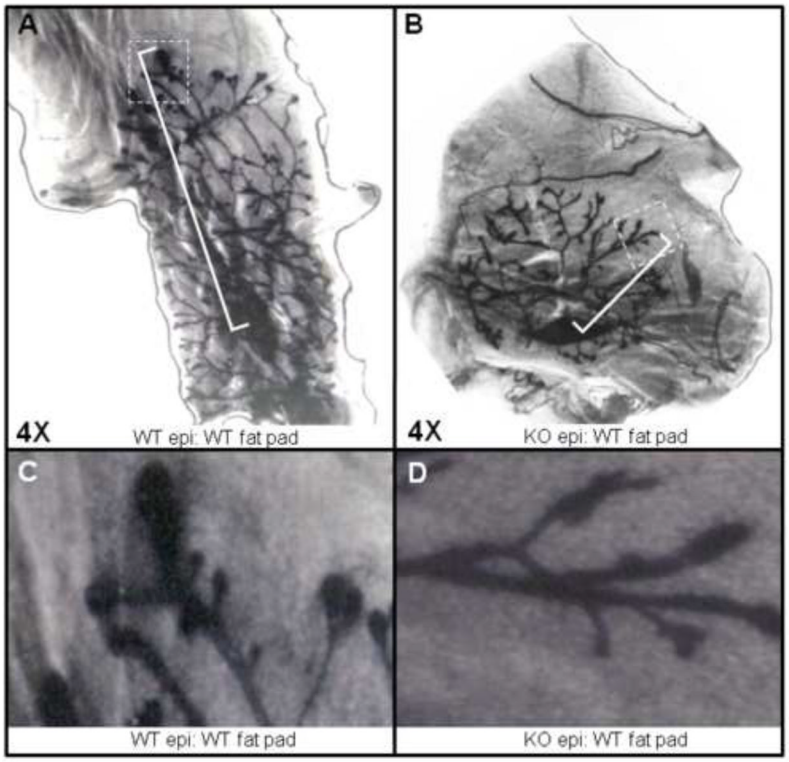

Fig. 4. Elongation defect is intrinsic to the MG

(A) WT epithelium transplanted into cleared fat pad of 3 week old WT mouse shows adequate elongation (n=3) as measured from center of transplanted epithelium to distal end of longest primary duct. Longest primary duct is bracketed and farthest distal end is boxed. **(B)** *Twsg1*$^{-/-}$ epithelium transplanted into cleared fat pad of 3 week old WT mouse shows impaired elongation (n=3) as measured from center of transplanted epithelium to distal end of longest primary duct. Longest primary duct is bracketed and farthest distal end is boxed. **(C)** Magnified view of transplanted WT distal ends. **(D)** Magnified view of transplanted *Twsg1*$^{-/-}$ distal ends.

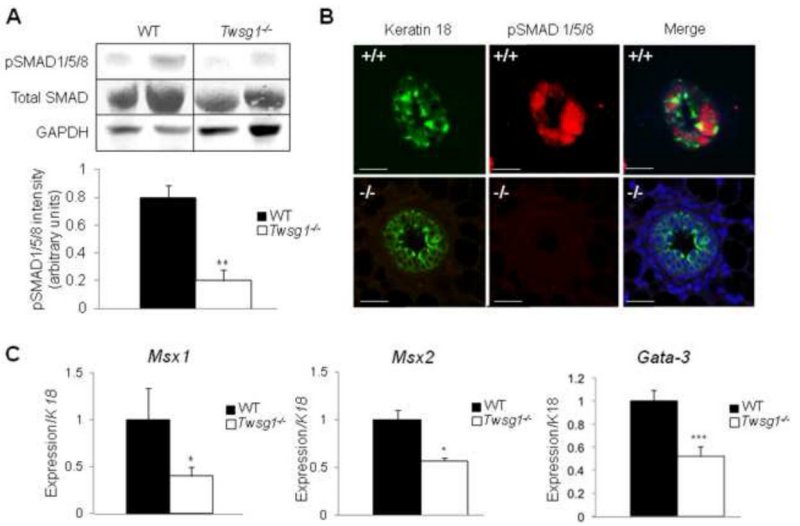

Fig. 5. BMP signaling is reduced in MGs from *Twsg1*$^{-/-}$ animals

(A) Western blot, showing two representative samples per group, detecting the levels of total SMAD, pSMAD 1/5/8 and GAPDH in MG lysates from WT and *Twsg1*$^{-/-}$ 6 week old virgins. Total SMAD was normalized to GAPDH and a ratio of SMAD to pSMAD1/5/8 was calculated; $p < 0.002$. **(B)** Immunofluorescence staining for epithelial marker keratin 18 (green) and pSMAD1/5/8 (red). pSMAD1/5/8 is absent in *Twsg1*$^{-/-}$ MGs **(C)** Q-PCR for BMP downstream targets, *Msx1, Msx2 and Gata3,* shows reduced expression in *Twsg1*$^{-/-}$ MGs. Scale bar 2 um.

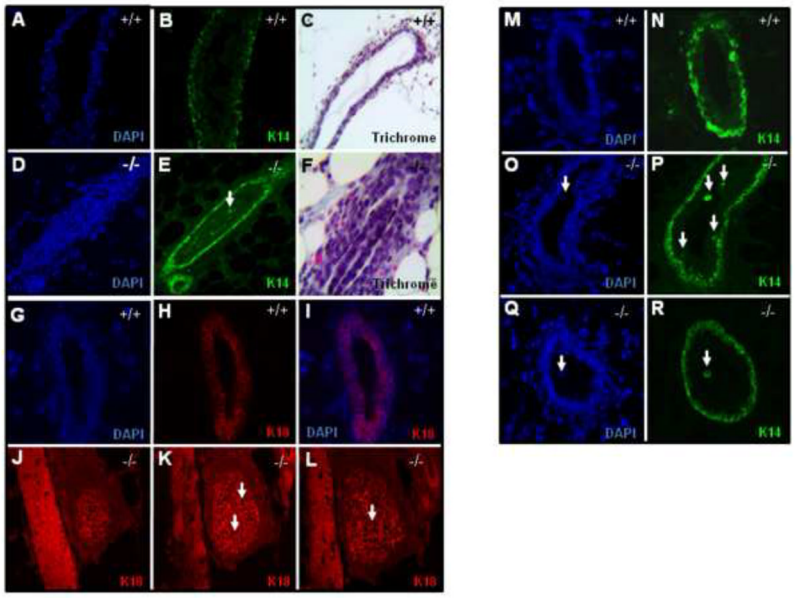

Fig. 6. *Twsg1*$^{-/-}$ MGs have abnormal epithelial organization, occluded lumens and cell shedding at puberty

(A–C) WT MGs **(D–F)** *Twsg1*$^{-/-}$ MGs stained with K14 have occluded lumens, which can be organized with a secondary myoepithelial compartment surrounding a mass of K14 negative cells. **(C,F)** Trichrome staining reveals cleared lumens of WT ducts and an organized cell mass within some lumens of the *Twsg1*$^{-/-}$ maturing duct. **(G–I)** WT ducts with a well formed lumen. (J–L) Using a blood vessel to mark the location within the MG, serial sections of an occluded *Twsg1*$^{-/-}$ duct were stained for K18. Not all the cells that occlude the lumen are K18 positive (arrows). **(M,N)** K14 stained WT mature ducts showing K14 positive cells in the basal compartment, but not the luminal compartment of the epithelium at puberty **(O,P)** K14 positive cells are found in the luminal compartment of *Twsg1*$^{-/-}$ mature ducts (arrow). **(Q,R)** Cell shedding in *Twsg1*$^{-/-}$ ducts. Cells shed into the lumen were preferentially K14 positive. All images were taken at 20X.

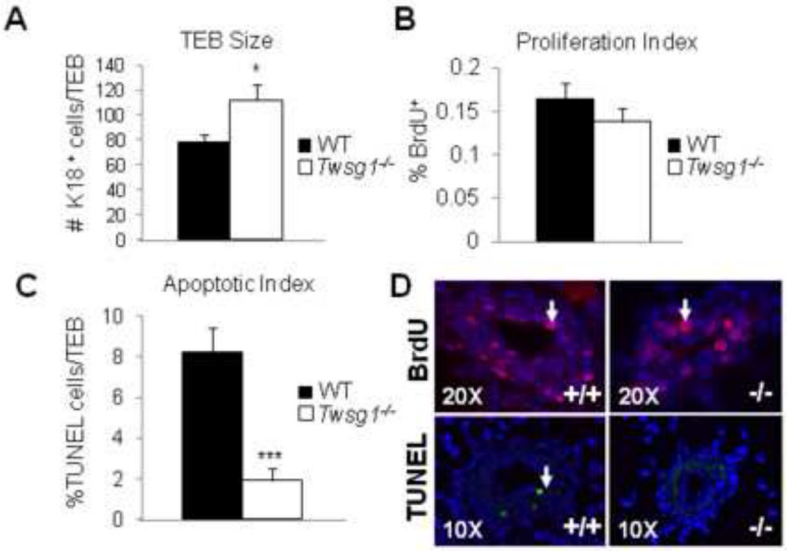

Fig. 7. *Twsg1*$^{-/-}$ TEBs show an increase in luminal epithelial (K18) cell number and a decrease in apoptosis

(A) K18 positive cells were counted within TEBs and compared between WT and *Twsg1*$^{-/-}$. A significant increase in cell number was observed in *Twsg1*$^{-/-}$ compared to WT. **(B)** BrdU positive cells were counted within the same compartment and no significant change in proliferation was observed. **(C)** TUNEL staining revealed a significant decrease in the number of apoptotic cells within the TEB of *Twsg1*$^{-/-}$ MGs. **(D)** Representative images for BrdU (pink), K18 (green) and TUNEL (green) staining. * $p<0.05$, *** $p<0.001$

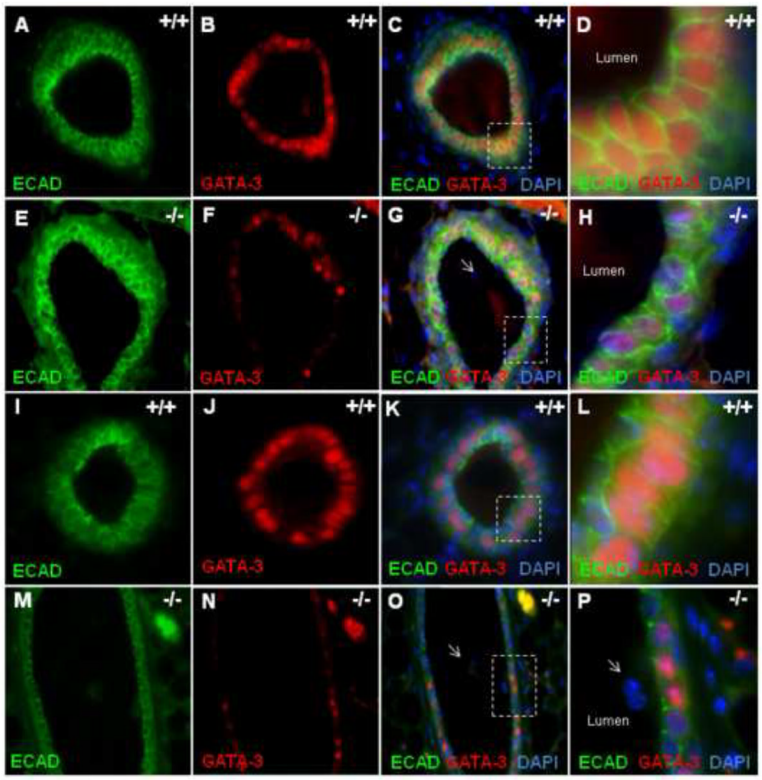

Fig. 8. GATA-3, required for luminal identity, is reduced in *Twsg1*$^{-/-}$ MGs

GATA-3 expression is reduced in *Twsg1*$^{-/-}$ MGs. ECAD was used to mark luminal epithelial cells and most ECAD positive cells in the WT TEB express GATA-3 (A–D) and mature duct (I–L) while the *Twsg1*$^{-/-}$ TEB (E–H) and mature duct (I–L) consist of a mosaic of GATA-3 positive and GATA-3 negative luminal cells. Most cells shed into the lumen are GATA-3 negative (P). All images were taken at 40X. Boxes in C, G, K, and O correspond to the magnified images in D, H, L, and P, respectively.

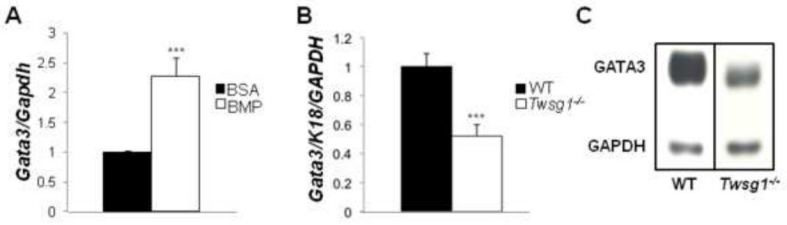

Fig. 9. GATA-3, required for luminal identity, is reduced in *Twsg1*$^{-/-}$ MGs

(A) *Gata-3* expression is significantly upregulated in HC11 cells that have been treated with BMP7 (50ng/ml). **(B)** *Gata-3* expression is significantly downregulated, in *Twsg1*$^{-/-}$ MGs from 6 week old virgin mice. **(C)** There is reduced GATA-3 protein in *Twsg1*$^{-/-}$ MGs (n=3) compared to WT (n=3).